Experimentally realizable devices for domain wall motion control

Sergey Savel'ev[1]**, Alexander Rakhmanov**[1,2] **and Franco Nori**[1,3]

[1] Frontier Research System, The Institute of Physical and Chemical Research (RIKEN), Wako-shi, Saitama 351-0198, Japan

[2] Institute for Theoretical and Applied Electrodynamics RAS, 125412 Moscow, Russia

[3] Center for Theoretical Physics, Department of Physics, Center for the Study of Complex Systems, The University of Michigan, Ann Arbor, MI 48109-1120, USA

E-mail: ssavelev@riken.jp, alrakhamov@mail.ru and nori@umich.edu

Abstract. Magnetic domain walls (MDWs) can move when driven by an applied magnetic field. This motion is important for numerous devices, including magnetic recording read/write heads, transformers and magnetic sensors. A magnetic film, with a sawtooth profile, localizes MDWs in discrete positions at the narrowest parts of the film. We propose a controllable way to move these domain walls between these discrete locations by applying magnetic field pulses. In our proposal, each applied magnetic pulse can produce an increment or step-motion for an MDW. This could be used as a shift register. A similarly patterned magnetic film attached to a large magnetic element at one end of the film operates as an XOR logic gate. The asymmetric sawtooth profile can be used as a ratchet resulting in either oscillating or running MDW motion, when driven by an ac magnetic field. Near a threshold drive (bistable point) separating these two dynamical regimes (oscillating and running MDW), a weak signal encoded in very weak oscillations of the external magnetic field drastically changes the velocity spectrum, greatly amplifying the mixing harmonics. This effect can be used either to amplify or shift the frequency of a weak signal.

Contents

1. Introduction

The very fast growth of information technology requires novel approaches to information storage, control and manipulation. Most magnetic memory devices store information by setting either up or down the magnetization of small magnetic particles or individual domains in magnetic films (see e.g. [1]–[6]). Such systems can be driven either by polarized currents (see e.g. [7]–[11]) or by magnetic fields generated by external sources [2, 4, 12].

Nonlinear logical devices (e.g. [13]) operating at room temperature attract considerable interest [1] because these do not require expensive cryogenics (in contrast to superconducting devices). In the present context, we focus on a magnetic domain wall (MDW) moving through a periodically patterned film and driven by magnetic field pulses. This motion can be mapped to the motion of an overdamped particle within a wide range of parameters, covering many possible applications [14]. Recently, the motion of tiny particles in periodic ratchet-like potentials has inspired a new generation of solid-state devices [16]–[20] and here we study how these ideas could be used for magnetic (relatively thick) films with an external magnetic field perpendicular to the film plane. The case of thin films, with magnetic fields along the film plane, has been studied in [21]. Using sawtooth-shaped ferromagnetic slabs or films, we propose set-ups for controllable MDW step motors (or shift-registers) and logic gates. In addition, we also drive the MDW to its bistable point (between oscillating and running MDW motion-solutions) with a weak signal, drastically changing the velocity spectrum of the MDW. This can be used as a weak-signal frequency-shifter and signal amplifier.

2. Magnetic domain wall (MDW)

We consider a soft ferromagnetic slab or film patterned with many triangles in the sawtooth shape shown in figure 1(a). The MDW separates regions having different orientations of the magnetization. This wall can be shifted from one minimum-thickness location to another one by applying an external magnetic field pulse. We assume that the easy axis (y-axis in figure 1) for the magnetization is perpendicular to the film plane. We also assume that the magnetic anisotropy field H_a is not small. If the film is sufficiently elongated along the y-direction (see figure 1), the magnetization vector points along the easy axis (i.e., along the y-axis) and domain walls should also be parallel to this axis. For this case, we can neglect the effect of stray fields.

Institute *of* **Physics** 🇩 DEUTSCHE PHYSIKALISCHE GESELLSCHAFT

The linear energy density $E(x)$ of the film (slab) in the externally applied magnetic field $H_e(t)$ along the y-direction (see figure 1) can be written as

$$E(x) = E_W l(x) L_y - 2M H_e(t) L_y \int_0^x l(x') \, \mathrm{d}x', \tag{1}$$

where x is the location of the domain wall, E_W is its energy per unit area, $l(x)$ is the variable film width, L_y is the constant film thickness, and M is the film magnetization. The second term on the right-hand-side of equation (1) is the usual Zeeman energy. The energy E_W of the domain wall can be expressed as $E_W = \gamma M^{3/2} H_a^{1/2} l_{\text{exchange}}$, where $\gamma \sim 1$–10 and l_{exchange} is the exchange length. The approximations discussed here have been successfully used [14] for describing MDW motion in different systems. Thus, it should also be applicable for our problem, at least qualitatively.

The external magnetic field $H_e(t)$ drives the wall in the patterned metal film according to the usual dynamical equation: friction force $= -\mathrm{d}E(x)/\mathrm{d}x$, which can be rewritten as

$$\beta \dot{x} = -\frac{E_W}{l(x)} \frac{\mathrm{d}l(x)}{\mathrm{d}x} + 2M H_e(t) - F_{\text{pin}} \frac{\dot{x}}{|\dot{x}|} \quad \text{for } \dot{x} \neq 0. \tag{2}$$

Here, $\dot{x} = \mathrm{d}x/\mathrm{d}t$. For $\dot{x} = 0$, the position of the domain wall does not change with time and we should find the time at which the domain wall starts to move. The friction force per unit area acting on the wall comes from two contributions [14]:

 (i) the eddy current friction $\beta \dot{x} l(x) L_y$ with $\beta = \frac{\gamma_1 (2\pi M)^2 L_y}{\rho c^2}$; and

(ii) the domain-wall coercive (pinning) force $-F_{\text{pin}} l(x) L_y \frac{\dot{x}}{|\dot{x}|}$ with coercive force per unit area F_{pin} of the MDW.

Here, ρ is the film's electrical resistivity and γ_1 is a constant of the order of unity, which depends on the sample geometry. Note that the approximation used for the eddy current friction is correct, when the skin depth is larger than the thickness L_y. This results in a limitation of the driving frequency as $\omega/2\pi \lesssim 10\,\text{MHz}$ for films with μm-size thickness. In equation (2), we omit the inertia term: this is usually valid up to several tens of GHz. In dimensionless units, equation (2) is reduced to

$$\dot{\mathcal{X}} = -\frac{l'(\mathcal{X})}{l(\mathcal{X})} + h(\tau) - f_p \frac{\dot{\mathcal{X}}}{|\dot{\mathcal{X}}|}, \tag{3}$$

where $\mathcal{X} = x/x_0$, $\dot{\mathcal{X}} = \mathrm{d}\mathcal{X}/\mathrm{d}\tau$, $\tau = t/t_0$, a prime denotes $\mathrm{d}/\mathrm{d}\mathcal{X}$, $h(t) = 2M H_e(t) x_0/E_W$, $f_p = F_{\text{pin}} x_0/E_W$. Here, the spatial scale x_0 is the period of sawtooth structure (figure 1) and $t_0 = \beta x_0^2/E_W$ is the characteristic damping time.

3. Controllable MDW step-motor or shift-register

Under steady-state conditions, the MDWs in the film shown in figure 1 can be located only at certain discrete positions, corresponding to the narrowest parts of the patterned film (e.g., red dashed lines in figure 1). This would occur if the sawtooth profile were steep enough in order for the restoring force (per unit area) to overcome the coercive force, $|l'(\mathcal{X})|/l(\mathcal{X}) > f_p$. When the driving magnetic field pulse $H(t)$ shown in figure 1 is applied, the domain wall can be
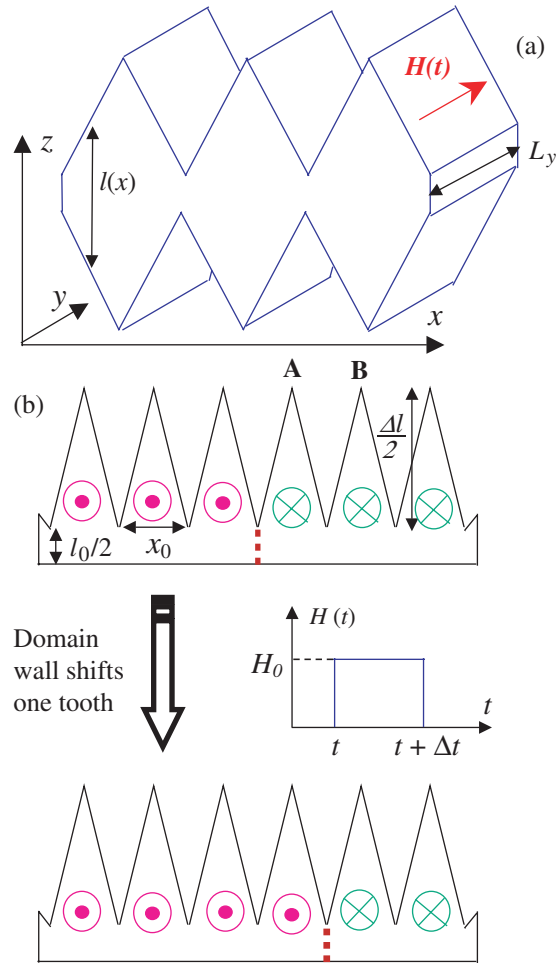
Figure 1. (a) A 3D-sketch of the sample, indicating the height $l(x)$ and width L_y. Note that the sample is mirror-symmetric along the x-direction, and thus, hereafter, we only draw the top part, to save space. (b) Schematic diagram of a MDW (red dashed vertical line) moving in a triangular-patterned film (here we only show its upper half). The domain-wall motion is easily controllable and robust to small variations of the magnetic field pulse, e.g., possible errors in either the duration Δt or the amplitude H_0 of the pulses (see text). These pulses can be generated by an external solenoid magnet (not shown here).

shifted from one minimum-thickness position to another. For a rectangular pulse of the applied magnetic field, equation (3) can be integrated exactly. This allows us to derive the times, τ^+ and τ^-, for the transitions of the domain wall from a minimum to the following maximum (τ^+) and from a maximum to the following minimum (τ^-):

$$\tau^{\pm} = \int_0^{1/2} \frac{\mathrm{d}\mathcal{X}}{h_0 - f_p \mp l'(\mathcal{X})/l(\mathcal{X})}. \tag{4}$$

Here, we introduce the dimensionless pulse amplitude $h_0 = 2MH_0x_0/E_W$. When deriving (4), we assume a symmetric (e.g., isosceles triangles) sawtooth profile of the film. Hereafter,

$$\tilde{h} \equiv h_0 - f_p = \text{driving force} - \text{coercive force} \tag{5}$$

denotes the 'effective depinning drive'. For a piecewise-linear structure, shown in figure 1, these transition times can be explicitly written as

$$\tau^{\pm} = \frac{1}{2\tilde{h}} \pm \frac{1}{\tilde{h}^2} \ln\left[1 + \frac{\tilde{h}\Delta l}{\tilde{h}l_0 \mp 2\Delta l}\right], \tag{6}$$

where we use the expression $l(\mathcal{X}) = l_0 + 2\,\mathcal{X}\,\Delta l$ for $\mathcal{X} < 1/2$ (i.e., from the minimum to the following maximum of the sawtooth profile). The domain wall cannot be shifted from its initial position, if the dimensionless magnetic field pulse $h(t)$ has an amplitude h_0 smaller than the threshold value

$$h_{\text{onset}} = f_p + \frac{2\Delta l}{l_0}. \tag{7}$$

At stronger pulses, the wall can be shifted to any desired number N of steps by changing the duration Δt of the pulse [15]:

$$N\tau^+ + (N-1)\tau^- < \frac{\Delta t}{t_0} < (N+1)\tau^+ + N\tau^-. \tag{8}$$

It is important to emphasize the robustness of this controllable step motor: due to the discrete equilibrium positions of the domain wall, we can shift it an exact integer number of steps, even though the pulse duration is established within an accuracy of about $(\tau^+ - \tau^-)$.

4. XOR logic gate

The nucleation and propagation of domain walls in the patterned sawtooth thick film (slab) can be used for the design of logic devices. Partly motivated by [13], here, we propose the asymmetric magnetic structure shown in figure 2: a large (e.g. rectangular) element is attached to one of the ends of the sawtooth structure. Using this device, we can construct an XOR logic gate (see the table at the bottom of figure 2). The inputs of this device are: the direction of an externally applied dc magnetic field and the direction of the magnetization of the large magnetic element, while the output is the motion of MDW, which generates the electric field.

Figure 3 shows the initialization and operation of this gate. The large pulse of the externally applied magnetic field magnetizes the whole structure either up (for a logic state '1') or down (for a logic state '0'). Afterwards, we combine both the zero average ac field $H_{ac}(t)$ and a dc bias field H_{dc}. For example, let us consider rectangular ac pulses with temporal period T:

$$H_{ac}(t) = H_{ac}(t + T);$$
$$H_{ac}(t) = H_0 \quad \text{for } t < T/2 \quad \text{and}$$
$$H_{ac}(t) = -H_0 \quad \text{for } t > T/2. \tag{9}$$

Institute *of* **Physics** ⏀ DEUTSCHE PHYSIKALISCHE GESELLSCHAFT

Input 1:
$H_{dc} > 0$ = "1"
$H_{dc} < 0$ = "0"

H_{dc}

Drive:
$H_{ac}(t)$

Input 2:
M > 0 = "1"
M < 0 = "0"

M

Output : Domain wall motion.
No motion = "0";
Oscillations = "1"

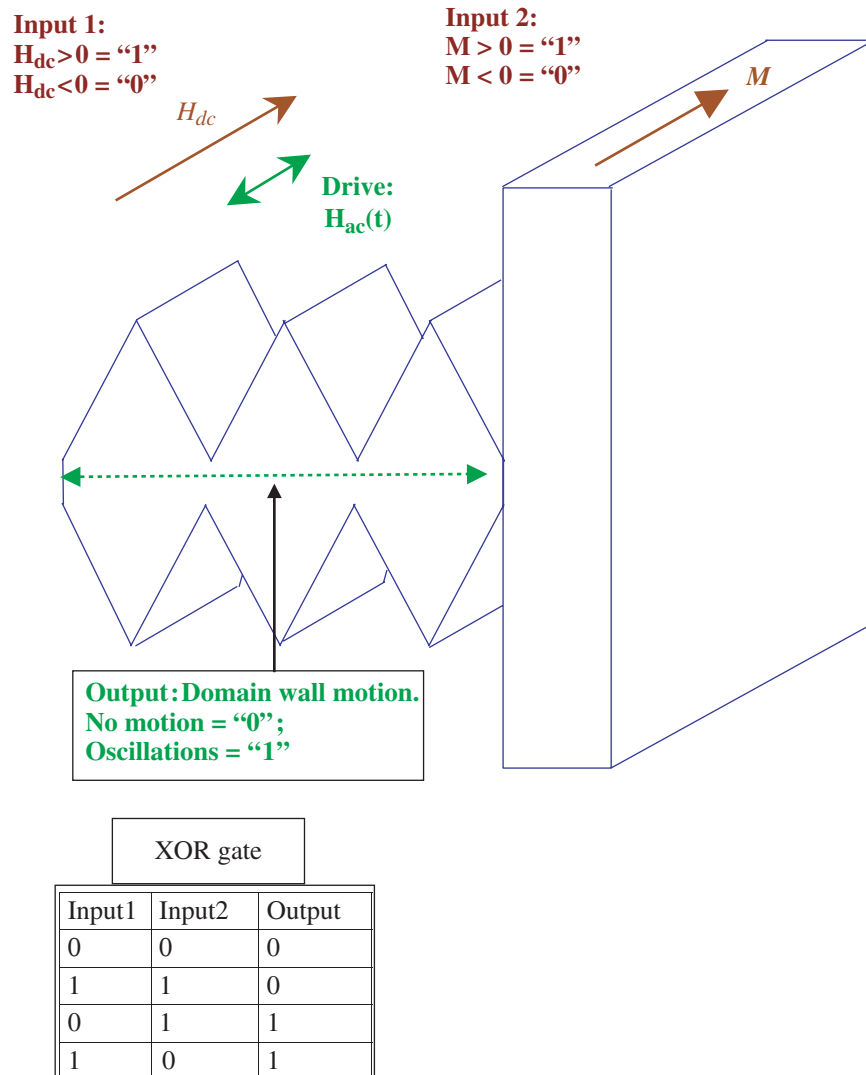| XOR gate		
Input1	Input2	Output
0	0	0
1	1	0
0	1	1
1	0	1

Figure 2. Geometry of a magnet slab for an XOR gate, also showing the inputs and output of the device.

We can assign the other state '1' for a positive H_{dc} and '0' for a negative H_{dc}. We can always choose an ac signal, so that $H_0 > |H_{dc}|$ and $H_0 - |H_{dc}| < H_c < H_0 + |H_{dc}|$, where H_c is the threshold field for domain wall nucleation at the open end of the sawtooth structure. Due to a strong shape anisotropy, the magnetization reversal field H_{c1} of the large attached element is higher than both H_c and $H_0 + |H_{dc}|$. If both states coincide ('1' + '1') or ('0' + '0'), the magnetization reversal process does not occur (output is '0'). Indeed, when the ac magnetic field direction is opposite to the direction of the film magnetization, the total field $H_0 - |H_{dc}|$ is not enough to create a domain wall at the open end. For the cases when ('1' + '0') or ('0' + '1'), the dc field assists the ac field ($H_0 + |H_{dc}|$) to nucleate the domain with opposite magnetization with respect to the magnetization of the large element. Thus, when both states are different, ('1' + '0') or ('0' + '1'), the nucleated domain wall moves back and forth inside the structure. This produces a magnetic response attributed to a new state '1' and could be measured. The amplitude of the output signal depends on the duration of the ac pulses. Therefore, this device operates as an XOR logic element.
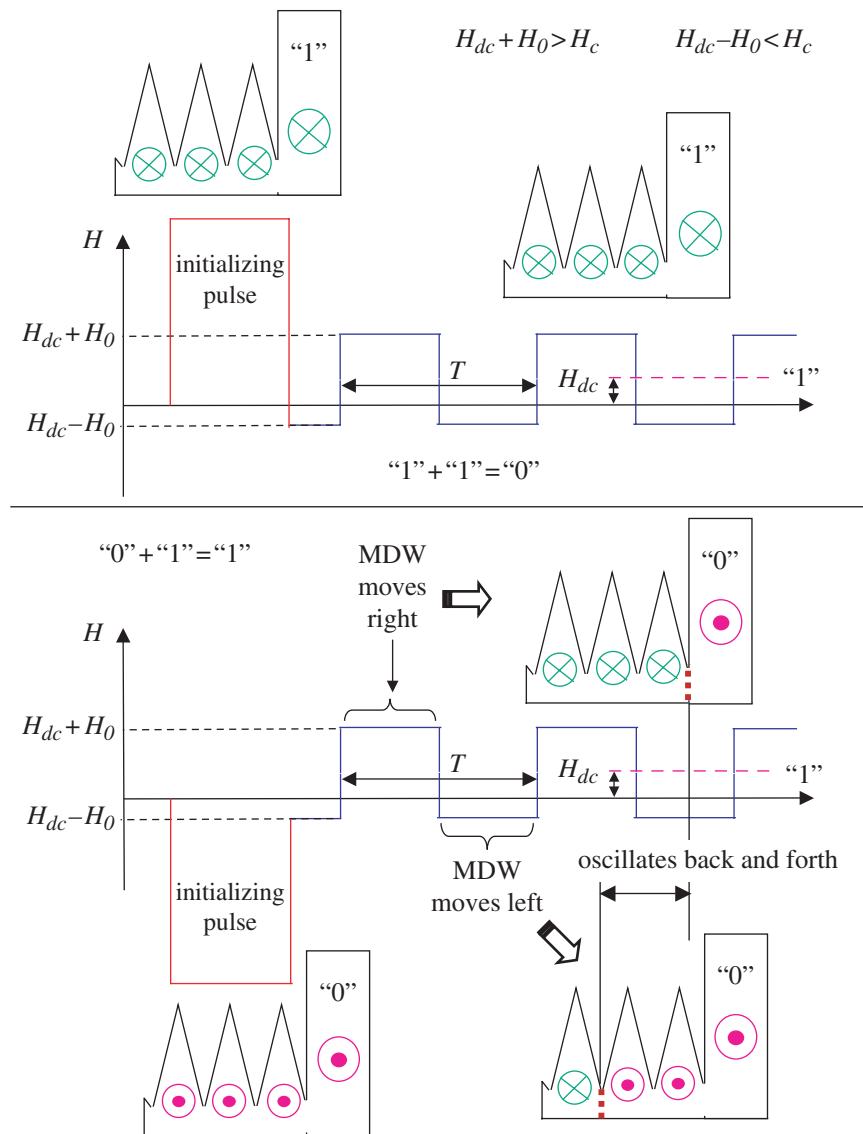
Figure 3. Schematic diagram of a magnetic logic gate operation. When applying a magnetic field, the entire patterned magnetic sample, including the large magnetic element, can be set to either its '0' or '1' state. This structure can work as an XOR gate if both an ac and dc magnetic fields are applied: $H_{dc} + H_{ac}(t)$. The inputs of the XOR gate are: (1) an applied dc field, and (2) the magnetization of the larger part of the structure. An ac field is added to start the XOR operation. The output can be either 'zero' (no domain wall) or 'one' (a domain wall is nucleated in the sample and oscillates). This MDW oscillation corresponds to the 'one' output state and can generate a voltage in a pick-up coil. Thus, the moving domain wall exists either for $H_{dc} > 0$ and state '1' or $H_{dc} < 0$ and state '0'.

5. Frequency-shifter and signal amplifier

Amplification of a weak signal is an important process in many physical and biophysical systems, as well as for applications (see e.g. [22]). A possible approach to amplification is to use

a nonlinear device near its bistability point. For instance, stochastic resonance (SR) [23] in such bistable systems utilizes noise to amplify a weak signal. Even though this effect has been used [23] for the amplification of signals in some settings, SR offers a rather limited controllability, since it has only one adjustable parameter: the noise strength. Here, we present an alternative deterministic (in contrast to stochastic resonance [23, 24] and diffusion amplification [25]) method of signal amplification in nonlinear devices by applying an additional periodic driving with rather large amplitude with respect to a weak drive. By mixing these two signals, we can sufficiently amplify the weak one and shift its frequency to a desirable range [26]. This effect exhibits a threshold behaviour and occurs if the strong drive brings the system close to a bistable point. A MDW in an asymmetric sawtooth profiled film is a physical system which is appropriate to observe this effect.

For simulations, we use equation (2), in which we neglect the coercive force (pinning) ($f_p = 0$) and assume

$$h(t) = a \cos(\omega_1 \tau) + \varepsilon \cos(\omega_2 \tau). \tag{10}$$

Thus, we derive

$$\dot{\mathcal{X}} = -\frac{\partial u}{\partial \mathcal{X}} + a \cos \omega_1 \tau + \varepsilon \cos \omega_2 \tau. \tag{11}$$

Here $u = \log[l(x)/x_0]$, the studied asymmetric potential $u(x)$ is depicted in the inset of figure 4(a), a is the strong drive amplitude of the external field, while $\varepsilon \ll a$ is a weak signal encoded as a weak oscillation of $h(t)$. We numerically obtain the MDW coordinate $\mathcal{X}(\tau)$ and the velocity $\dot{\mathcal{X}}(\tau)$ and then calculate the Fourier transform $\dot{\mathcal{X}}(\omega)$ of $\dot{\mathcal{X}}(\tau)$. Note that the output $\dot{\mathcal{X}}(\omega)$ can be directly measured in experiments, since it is proportional to the electric field generated.

On slowly increasing the amplitude of the ac driving force, we observed that the confined motion of the MDW near a potential minimum is eventually changed to a directed (rectified) motion. When the driving force extends far beyond a rectification threshold, called here the bistable point, the typical Fourier transform $\dot{\mathcal{X}}(\omega)$ (figure 4(c)) exhibits a set of peaks corresponding to the driving frequency ω_1 and its harmonics $n\omega_1$, where n is an integer. Harmonics, $n \neq 1$, occur due to the nonlinearity of the potential. The output $\dot{\mathcal{X}}(\omega)$ is practically 'independent' of the presence or absence of a small additional force $\varepsilon \cos \omega_2 \tau$: the signal is too weak to affect the motion of the MDW. The same situation occurs when the driving force is small enough and the weak signal is too small to assist the MDW to overcome potential barriers.

The picture changes significantly within a narrow window of driving amplitudes and frequencies near the rectification threshold. From the non-amplified response (e.g. shown by the arrow in figure 4(c)) for either large or small driving a, its spectrum suddenly changes to the amplified output $\mathcal{X}$ (shown in figures 4(a) and (b)) for driving very near the bistable point. Indeed, near the bistable point, many additional peaks in $\dot{\mathcal{X}}(\omega)$ appear. The additional peaks correspond to the combinations $n\omega_1 + m\omega_2$, where n, m are integers (either negative or positive). The heights of the peaks slowly decrease with increasing n, m and for the first several peaks are of the order of the main peaks corresponding to $n\omega_1$.

In strong contrast to the mixing signal reported in [15] and the two-signal SR [24], both of which only occur for commensurate ω_1 and ω_2 and are controlled by the relative phases of two applied signals, the amplification discussed here occurs for both commensurate and incommensurate drives. Also, the spectrum $\dot{\mathcal{X}}(\omega)$ studied here exhibits different properties
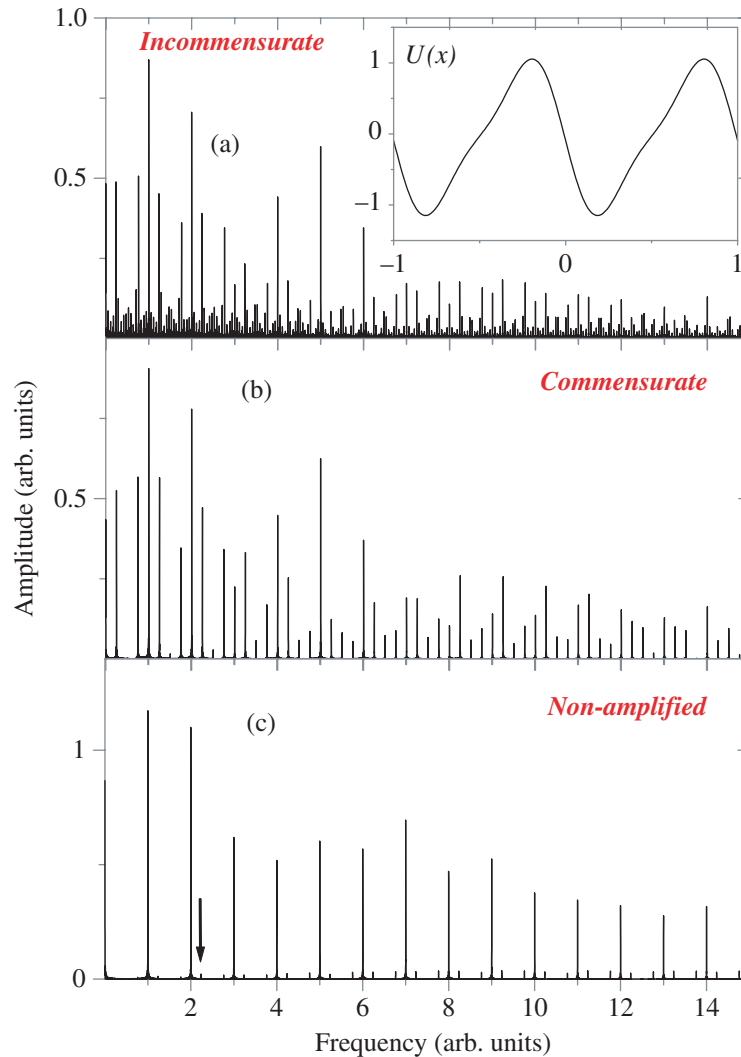
Figure 4. The Fourier spectrum of the velocity of (a) a MDW in a ratchet potential, shown in the inset of (a), for the driving amplitude $a = 6.72$ (which is close to a bistable point between confined and running solutions) and frequency $\omega_1 = 2\pi$. The weak signal amplitude is chosen to be $\varepsilon = 0.03$ and $\omega_2 = \sqrt{5}\omega_1$. Even though the weak signal is $\lesssim 0.5\%$ of the strong force, the produced harmonic amplitudes are of the order of the main drive. (b) Same as in (a) for commensurate frequencies, $\omega_2 = (9/4)\omega_1 = 2.25\,\omega_1$ and close to the bistable point $a = 6.72$. Even though the weak signal frequency is close to the incommensurate frequency in (a), the dense set of weak peaks disappears for the commensurate case (b). (c) Same as in (b), but with $a = 7$, away from the bistable point: the response is given by the strong drive and its harmonics (the weak signal plays no role here).

for commensurate, $\omega_1/\omega_2 = p/q$, and incommensurate, $\omega_1/\omega_2 \neq p/q$, input frequencies with integer p and q (figures 4(a) and 4(b)). Namely, a series of well-separated peaks appear for commensurate frequencies; otherwise, a dense set of smaller peaks occurs in addition to the large peaks in $\mathcal{X}(\omega)$. This unusual amplification is observed within a few per cent of the driving amplitude a or frequency ω_1.

Institute *of* **Physics** Φ DEUTSCHE PHYSIKALISCHE GESELLSCHAFT

6. Conclusions

We proposed various ways to precisely control the motion of domain walls in patterned magnetic films. These could be used for making the controllable step motors for moving domain walls (e.g. for magnetic shift registers) and for logic gates. These devices can be operated at room temperature, since thermal noise is negligible with respect to their characteristic energies involved.

For an asymmetric sawtooth magnetic film placed in an external magnetic field with two frequencies, we propose a novel general mechanism for large nonlinear signal amplification and shifting the output response to a desirable frequency.

Acknowledgments

References

[1] Mee C D and Daniel E D 1996 *Magnetic Storage Handbook* (New York: McGraw-Hill)
[2] Weller D 2004 *Nature* **428** 831
[3] Koo H, Krafft C and Gomez R D 2002 *Appl. Phys. Lett.* **81** 862
[4] Gerrits T *et al* 2002 *Nature* **418** 509
[5] Kikuchi N 2001 *J. Appl. Phys.* **90** 6548
[6] Boeve H *et al* 1999 *J. Appl. Phys.* **85** 4779
[7] Kimura T *et al* 2003 *J. Appl. Phys.* **94** 7947
[8] Kimura T *et al* 2003 *J. Appl. Phys.* **94** 7266
[9] Jiang Y *et al* 2004 *Nature Materials* **3** 361
[10] Yamaguchi A *et al* 2004 *Phys. Rev. Lett.* **92** 077205
[11] Tatara G and Kohno H 2004 *Phys. Rev. Lett.* **92** 086601
[12] Saitoh E *et al* 2004 *J. Appl. Phys.* **95** 1986
[13] Cowburn R P and Welland M E 2000 *Science* **287** 1466
[14] Gurevich A G and Melkov G A 1996 *Magnetization Oscillations and Waves* (Boca Raton, FL: CRC Press)
[15] Savel'ev S, Marchesoni F, Hänggi P and Nori F 2004 *Europhys. Lett.* **67** 179
     Savel'ev S, Marchesoni F, Hänggi P and Nori F 2004 *Eur. Phys. J.* B **40** 403
     Savel'ev S, Marchesoni F, Hänggi P and Nori F 2004 *Phys. Rev.* E **70** 066109
[16] Reimann P 2002 *Phys. Rep.* **361** 57
     Astumian R D and Hänggi P 2002 *Phys. Today* **55** (11) 33
     Linke H 2002 *Appl. Phys.* A **75** 167 (special issue on Brownian motors)
     Wambaugh J F *et al* 1999 *Phys. Rev. Lett.* **83** 5106
     Marchesoni F, Zhu B Y and Nori F 2003 *Physica* A **325** 78
     Zhu B Y, Marchesoni F and Nori F 2003 *Physica* E **18** 318
     Zhu B Y, Marchesoni F and Nori F 2003 *Physica* E **18** 322
     Zhu B Y, Marchesoni F and Nori F 2004 *Phys. Rev. Lett.* **92** 180602
     Zhu B Y, Marchesoni F, Moshchalkov V V and Nori F 2003 *Phys. Rev.* B **68** 014514
     Zhu B Y, Marchesoni F, Moshchalkov V V and Nori F 2003 *Physica* C **388** 665
     Zhu B Y, Marchesoni F, Moshchalkov V V and Nori F 2004 *Physica* C **404** 260

Institute *of* **Physics** ⚛ DEUTSCHE PHYSIKALISCHE GESELLSCHAFT

[17] Savel'ev S and Nori F 2002 *Nature Materials* **1** 179
[18] Villegas J E, Savel'ev S, Nori F, Gonzalez E M, Anguita J V, García R and Vicent J L 2003 *Science* **302** 1188
[19] Savel'ev S, Marchesoni F and Nori F 2003 *Phys. Rev. Lett.* **91** 010601
 Savel'ev S, Marchesoni F and Nori F 2004 *Phys. Rev. Lett.* **92** 160602
 Savel'ev S, Marchesoni F and Nori F 2004 *Phys. Rev.* E **70** 061107
 Savel'ev S, Marchesoni F and Nori F 2005 *Phys. Rev.* E **71** 011107
[20] Denisov S I, Denisova E S and Hänggi P 2005 *Phys. Rev.* E **71** 016104
[21] Savel'ev S, Rakhmanov A and Nori F, unpublished
[22] Gomperts B D, Kramer I M and Tatham P E R 2002 *Signal Transduction* (New York: Academic)
[23] Gammaitoni L, Hänggi P, Jung P and Marchesoni F 1998 *Rev. Mod. Phys.* **70** 223
 Wellens T, Shatokhin V and Buchleitner A 2004 *Rep. Prog. Phys.* **67** 45
[24] Gammaitoni L, Löcher M, Bulsara A, Hänggi P, Neff J, Wiesenfeld K, Ditto W and Inchiosa M E 1999 *Phys. Rev. Lett.* **82** 4574
[25] Reimann P, Van den Broeck C, Linke H, Hänggi P, Rubi J M and Pérez-Madrid A 2001 *Phys. Rev. Lett.* **87** 010602
[26] Savel'ev S, Rakhmanov A and Nori F, unpublished